Biochem. J. (1994) 304, 895–902 (Printed in Great Britain)

The α-5 segment of *Bacillus thuringiensis* δ-endotoxin: *in vitro* activity, ion channel formation and molecular modelling

Ehud GAZIT,* Diana BACH,* Ian D. KERR,† Mark S. P. SANSOM,† Nor CHEJANOVSKY‡ and Yechiel SHAI*§

* Department of Membrane Research and Biophysics, Weizmann Institute of Science, Rehovot, 76100 Israel, † Laboratory of Molecular Biophysics, University of Oxford, The Rex Richards Building, South Parks Road, Oxford, OX1 3QU, U.K. and ‡ Department of Entomology, ARO, The Volcani Center, Bet Dagan, Israel

A peptide with a sequence corresponding to the highly conserved α-5 segment of the Cry δ-endotoxin family (amino acids 193–215 of *Bacillus thuringiensis* CryIIIA [Gazit and Shai (1993) Biochemistry **32**, 3429–3436]), was investigated with respect to its interaction with insect membranes, cytotoxicity *in vitro* towards *Spodoptera frugiperda* (Sf-9) cells, and its propensity to form ion channels in planar lipid membranes (PLMs). Selectively labelled analogues of α-5 at either the N-terminal animo acid or the ε-amine of its lysine, were used to monitor the interaction of the peptides with insect membranes. The fluorescent emission spectra of the 7-nitrobenz-2-oxa-1,3-diazole-4-yl (NBD)-labelled α-5 peptides displayed a blue shift upon binding to insect (*Spodoptera littoralis*) mid-gut membranes, reflecting the relocation of the fluorescent probes to an environment of increased apolarity, i.e. within the lipidic constituent of the membrane. Moreover, mid-gut membrane-bound NBD-labelled α-5 peptides were protected from enzymic proteolysis. Functional characterization of α-5 has revealed that it is cytotoxic to Sf-9 insect cells, and that it forms ion channels in PLMs with conductances ranging from 30 to 1000 pS. A proline-substituted analogue of α-5 is less cytolytic and slightly more exposed to enzymic digestion. Molecular modelling utilizing simulated annealing via molecular dynamics suggests that a transbilayer pore may be formed by α-5 monomers that assemble to form a left-handed coiled coil of approximately parallel helices. These findings further support a role for α-5 in the toxic mechanism of δ-endotoxins, and assign α-5 as one of the transmembrane helices which form the toxic pore. The suggested role is consistent with the recent finding that cleavage of CryIVB δ-endotoxin in a loop between α-5 and α-6 is highly important for its larvicidal activity [Angsuthanasombat, Crickmore and Ellar (1993) FEMS Microbiol. Lett. **111**, 255–262].

INTRODUCTION

The Gram-positive bacterium *Bacillus thuringiensis* (Bt) produces insecticidal crystalline protein inclusions during sporulation (Höfte and Whiteley, 1989). The insecticidal activity of these inclusions is attributed to their major components, the various δ-endotoxins. It has been suggested that δ-endotoxins are composed of two major domains, one involved in receptor binding, which might explain the high specificity of the various δ-endotoxins to specific species, and the other is responsible for their toxic effects (Ge et al., 1989; Van Rie et al., 1990; Lee et al., 1992). It has been hypothesized that receptor binding causes conformational changes, that lead to the exposing of the δ-endotoxin's cytotoxic domain (Li et al., 1991; Aronson, 1993). The subsequent interaction of the toxic domain with target cell membranes facilitates pore formation in the mid-gut epithelium of insects. This results in osmotic shock to the cells and ultimately causes the insect's death (Sacchi et al., 1986; Knowles and Ellar, 1987). It has been shown that different δ-endotoxins form single ion channels in planar lipid bilayers (Slatin *et al.*, 1990; Schwartz *et al.*, 1993) and that they change the ion flux of cultured insect cells (Schwartz et al., 1991), reflecting the permeation properties of the toxins. The channels exhibit several conductance levels ranging from 100 pS to about 4000 pS. Although not yet proven, the ion channel activity of δ-endotoxin may be explained in terms of a model in which some of the α-helices of the toxin domain form transmembrane amphiphilic α-helices, which can assemble in bundles in which outwardly-directed hydrophobic surfaces interact either with other hydrophobic transmembrane segments or with the lipid core of the membrane, while inwardly facing hydrophilic surfaces produce an aqueous, ion-conducting pore (Inouye, 1974; Greenblatt et al., 1985; Guy and Seetharamulu, 1986; Lear et al., 1988; Sansom, 1991). Indeed, X-ray crystallography of the cryIIIA δ-endotoxin has revealed that the pore-forming domain contains seven α-helices, one of which, a 23 amino acid amphiphilic α-helix (amino acid residues 193–215, termed α-5), is highly conserved within the δ-endotoxin family (Li et al., 1991). This α-5 region is thought to play a major role in the toxic activity of δ-endotoxin both because of its predicted amphiphilic α-helical structure, which is characteristic of channel-forming peptides, and because various mutations in this region alter the toxic effect of the intact molecule (Ahmad and Ellar, 1990; Wu and Aronson, 1992). Furthermore, a cleavage site that is important for the activity of CryIVB δ-endotoxin has been found in the predicted loop between α5 and α6 helices (Angsuthanasombat et al., 1993). The occurrence and the location of this cleavage site, together with its role in larvicidal activity, further strengthen the hypothesis that α5 plays a major role in the toxic activity of δ-endotoxins, presumably by helping α-5 to interact with the insect membrane. We have shown that a synthetic peptide with sequence identical to α-5 adopts 58% α-helix structure in methanol, strongly interacts with model membranes,

Abbreviations used: Sf, *Spodoptera frugiperda*; PLM, planar lipid membrane; NBD-F, 4-fluoro-7-nitrobenz-2-oxa-1,3-diazole; Bt, *Bacillus thuringiensis*; TFA, trifluoroacetic acid; IPA, isopropyl alcohol; TFE, trifluoroethanol; P-α-5, Pro^{201}-α-5; DMSO, dimethyl sulphoxide; SA/MD, simulated annealing via restrained molecular dynamics.

§ To whom correspondence should be addressed.

permeates acidic phospholipid vesicles better than zwitterionic ones, and has lytic activity towards human erythrocytes (Gazit and Shai, 1993). These properties might be attributed either to membrane destruction, or to the ability of the peptide to penetrate the membrane and to form channels via aggregation of helices.

To support a role for α-5 in the toxic mechanism of δ-endotoxins, and as one of the transmembrane α-helices which may form the pore, we show here that: (i) the α-5 segment interacts with the mid-gut membrane of insects, embedded within them with its N-terminal part in a more hydrophobic environment than its C-terminal part; (ii) α-5 is protected from proteolytic digestion in its membrane-bound state slightly better than its Pro^{201}-substituted analogue; (iii) α-5 is cytotoxic to *Spodoptera frugiperda* (Sf-9) insect cells more than its Pro^{201}-substituted analogue; (iv) α-5 can form ion channels in planar lipid membranes (PLMs) with multiple conductance levels; and (v) molecular modelling studies based on intramembraneous aggregation of α-5 monomers suggest that a transbilayer pore may be formed by a left-handed coiled coil bundle of helices.

MATERIALS AND METHODS

Materials

BOC-Gly-PAM resin was purchased from Applied Biosystems (Foster City, CA, U.S.A.). BOC amino acids were obtained from Peninsula Laboratories (Belmont, CA, U.S.A.). Other reagents for peptide synthesis included trifluoroacetic acid (TFA) (Sigma), *N*,*N*-di-isopropylethylamine (Aldrich; distilled over ninhydrin), dicyclohexylcarbodiimide (Fluka), 1-hydroxybenzotriazole (Pierce) and dimethylformamide (peptide synthesis grade, Biolab, Israel). L-α-Phosphatidylcholine (type 4 S) was obtained from Sigma and further purified using the method of Kagawa and Racker (1971). NBD-F (4-fluoro-7-nitrobenz-2-oxa-1,3-diazole) and Trypan Blue were obtained from Sigma. Cholesterol (extra pure) was purchased from Merck (Darmstadt, Germany) and was recrystallized twice from ethanol. All other reagents were of analytical grade. Buffers and salt solutions were prepared using double glass-distilled water.

Peptide synthesis, fluorescent labelling and purification

The experimental procedure for the synthesis and fluorescent labelling of the peptides at their *N*-terminal amino acids was performed as described in detail elsewhere (Gazit and Shai, 1993). The labelling of the peptide with NBD at the ε-amino group of the lysine was performed under similar conditions. However, in that case an N-terminal acetylated peptide, that has been cleaved from the resin was used. The synthetic peptides were purified by reversed-phase h.p.l.c. on a C4 reversed-phase Vydac column (4.6 mm × 250 mm, 300 Å pore size). The column was eluted in 40 min, at a flow rate of 0.6 ml/min, using a linear gradient of 25–80 % acetonitrile in water, both containing 0.1 % TFA (v/v).

Preparation of insect mid-gut membranes

Mid-gut membranes were prepared from *Spodoptera littoralis* larvae. Larvae were chilled on ice for 15 min, then, upon dissection, the mid-guts were pulled gently from the larvae. Each mid-gut was opened by a longitudinal dissection and was rinsed free of the peritropic membrane and gut contents by several washes with a ice-cold buffer (300 mM mannitol/5 mM RGTA/17 mM Tris/HCl, pH 7.5). The isolated mid-guts were blotted and weighed, placed into a vial with a small amount of the buffer and frozen quickly in liquid nitrogen. The membranes were stored at −70 °C until use. Prior to their use, the membranes were slowly defrosted, vortexed, and homogenized.

Intrinsic fluorescence measurements

Changes in the fluorescence of NBD-labelled α-5 peptides were measured upon their binding to *S. littoralis* membranes. NBD-labelled peptides (0.2 nmol) were added to 2 ml of buffer (50 mM Na_2SO_4/25 mM Hepes/SO_4^{2-}, pH 6.8) and the emission spectra were recorded with a Perkin Elmer LS50B spectrofluorimeter, with excitation set at 468 nm (4 nm slit). A suspension of 20 μl of *S. littoralis* mid-gut homogenate (1.8 mg dry wt.) was added to the peptide-containing solutions, and the emission spectra were recorded after 2 min of incubation. The emission spectrum of the membranes alone was subtracted from the observed spectra in the presence of the peptides.

Enzymic digestion of membrane-bound peptide

NBD-labelled peptides (0.2 nmol) were dissolved in buffer (2 ml of 50 mM Na_2SO_4/25 mM Hepes/SO_4^{2-}, pH 6.8) and titrated against a dispersion of membrane until a plateau was observed (total amount of 1.8 mg dry wt.), thus ensuring that all the peptides were bound to the membranes. A 20 μl solution of proteinase-K (0.25 mg/ml) was then added and the fluorescence intensity as a function of time was obtained before and after addition of the enzyme. In a control experiment, NBD-α-5 (0.1 μM) was mixed with the enzyme prior to its addition to a solution containing the membranes. Experiments were repeated three times. Fluorescence intensities were recorded at room temperature in Perkin Elmer LS-50B and LS5 spectrofluorimeters, with excitation set at 470 nm, using a 10 nm slit, and with emission monitored at 530 nm, using a 5 nm slit. Measurements were performed in a 1 cm path-length quartz cuvette in a final reaction volume of 2 ml.

Ion channel measurements on PLMs

Planar bilayers were formed on the tip of glass pipettes using the method of Coronado and Latorre (1983). Micropipettes were pulled from borosilicate glass capillaries (A-M Systems, Everett, WA, U.S.A.) on a Kopf model 700C puller (Tujunga, CA, U.S.A.). The reference electrode was a calomel electrode in 3 M KCl connected to the bath solution with a glass bridge containing the same salt as in the dish. Bilayers were formed from a mixture of soybean lecithin and cholesterol (20 % w/w), dissolved in *n*-hexane at a concentration of 1.0 mg/ml. Lipid solution (1–2 μl) was introduced onto the surface (0.5 cm^2) of 300 or 600 μl of a salt solution (either 0.5 M NaCl or 0.5 M KCl, buffered with 5×10^{-3} M Hepes buffer, pH 7.4) in a glass dish with the micropipette tip placed in the solution. After evaporation of the organic solvent, the pipette was passed through the interface, allowing formation of a bilayer. After formation of the bilayers (electrical resistance was 5–20 GΩ), their stability was monitored for about 10 min at the highest potential chosen for single channel recording experiments. When a satisfactory degree of stability was achieved, i.e. no intrinsic conductance fluctuations were observed, a few microlitres of the peptide solution [freshly prepared in either isopropyl alcohol (IPA)/H_2O or in trifluoroethanol (TFE)/H_2O (1:1 v/v) at a concentration of about 500 μg/ml] were added to one side of the bilayer (virtual ground). Experiments were repeated 9 times. Electrical measurements were performed with an Axopatch-1D patch clamp apparatus (Axon Instruments, Foster City, CA, U.S.A.). Current flowing through the bilayers was recorded on an FM magnetic tape Hewlett Packard, Model 3694A. The experimental data obtained

were analysed off-line by replaying the recorded data from the tape through a low-pass filter at 100 Hz (Frequency Devices, Series 902, Haverhill, MA, U.S.A.) into an IBM PC AT computer and analysed with the Axotape and pClamp (version 5.5.1) programs (Axon Instruments).

Cell line and *in vitro* cytotoxic assay

Sf-9 cells were grown in TNM-FH medium (Hink, 1970; purchased from Sigma) containing 10% fetal calf serum, at 28 °C. The cells were spread over a 96-well dish (200 μl/well). Each well contained approx. 6×10^4 cells. Increasing amounts of α-5 or P-α-5 (Pro^{201}-α-5) (Gazit and Shai, 1993), dissolved in dimethyl sulphoxide (DMSO) were added to the cells and the viability was monitored. To perform toxicity kinetics measurements, 10 μg of α-5, or P-α-5, dissolved in DMSO, were added to the cells and the cytotoxic activity was monitored with time at room temperature. Viability was measured by Trypan Blue (0.1%, w/v) vital staining assay. In control experiments the peptide solvent alone was added to the cells.

Molecular modelling

Simulated annealing via restrained molecular dynamics (SA/MD) was carried out using XPLOR v3.1 (parameter set param19x.pro; Brünger, 1993) run on a DEC 3000 400 workstation. Molecular modelling was performed using QUANTA v3.2 (Molecular Simulations, Waltham, MA, U.S.A.) run on a Silicon Graphics (Mountain View, CA, U.S.A.) Indigo R3000 workstation, and diagrams of structures drawn using MolScript (Kraulis, 1991). Pore radii were estimated using HOLE (Smart et al., 1993). All auxiliary programs were written in Fortran 77.

Single δ-endotoxin α-5 helices were generated by SA/MD as previously described (Nilges and Brünger, 1991; Kerr and Sansom, 1993). Their amphiphilicity was analysed by examination of hydrophilic surface maps (Kerr and Sansom, 1993) and molecular hydrophobicity potentials (Brasseur, 1991). This analysis revealed that residues Q199 and D210 defined the centre of the hydrophilic face of the α-5 helix. Hexameric ($n = 6$) bundles of δ-endotoxin α-5 helices were generated in a manner similar to that described for parallel bundles of simple hydrophobic helices (Kerr et al., 1994). Briefly, Cα templates were generated corresponding to the α-carbon atoms of bundles of idealized α-helices packed such that the centres of the helices were at the apices of a regular hexagon with a side length of 9.4 Å. The helices were oriented within the bundle such that hydrophilic surface defined by the Cα atoms of residues Q199 and D210 pointed towards the central (pore) axis. All other main-chain and side-chain atoms were superimposed on the corresponding Cα atoms. Two alternative Cα templates were used: (a) a template with exactly parallel helices, i.e. $\Omega_{INIT} = 0°$ (where Ω is the helix crossing angle; Chothia et al., 1981); and (b) a template with adjacent helices crossed at $\Omega_{INIT} = +18°$, thus forming a left-handed coiled coil. Studies of Ala-20 and Leu-20 bundles have suggested that the latter is a stable packing arrangement for approximately parallel helices (Kerr et al., 1994), corresponding to 'ridges in grooves' packing of the side chains (Chothia et al., 1981). Each Cα template was used to generate an ensemble of 16 structures by SA/MD. During the final 5 ps burst of dynamics in the second stage of the SA/MD procedure, inter-helical distance constraints were employed in order to maintain approximate 6-fold symmetry about the bundle (z) axis. Two classes of restraint were employed: (a) '1–2' restraints between adjacent helices of the bundle; (b) '1–4' restraints between opposite helices of the bundle. In both cases restraints linked the centres of the two helices. The target distances for the two classes of restraints were 9.4 Å and 18.8 Å respectively. Studies on α-5 bundles generated without '1–4' restraints (results not shown) have suggested that omission of such restraints results in less symmetrical bundles of helices.

SA/MD calculations were performed in the absence of explicit solvent or bilayers. However, the electrostatic term was adjusted to allow for solvent screening within the pore (i.e. use of a distance-dependent dielectric), and the inter-helix restraints mimicked the effect of the bilayer in holding the helices in an approximately parallel orientation. Thus, the simulations represented an objective and automated protocol for satisfying the geometrical and steric requirements in packing together the helices into a bundle. Comparable approaches to modelling channel-forming peptides have been employed by, for example, Oiki et al. (1988a,b) and Lear et al. (1988).

RESULTS

To evaluate a role for the α-5 helix in δ-endotoxin activity and as a constituent of the pore formed by the toxin, a peptide whose sequence is identical to that of the α-5 helix segment of cryIIIA δ-endotoxin (residues 193–215), its Pro^{201} analogue (designated P-α-5) and its fluorescent analogues labelled with NBD either at its N-terminal amino acid or at Lys^{209} (part of which have been synthesized previously; Gazit and Shai, 1993), were synthesized and investigated for their *in vitro* activities and for their ability to form single channels in PLMs. That these channels may be energetically favoured was then supported utilizing molecular modelling. The sequences of the peptides are given in Table 1.

NBD fluorescence studies

The fluorophore NBD can be utilized for polarity and binding studies as its fluorescence spectrum reflects the environment in which it is located. Accordingly, the fluorescence emission spectra of NBD-labelled α-5 peptides and of NBD-aminoethanol, serving as a control, were monitored in aqueous solutions or in the presence of *S. littoralis* mid-gut membranes. NBD-α-5, NBD-P-α-5, NBD-Lys-α-5, and NBD-aminoethanol exhibited fluorescence emission maxima at 549 nm in buffer (Table 2), in agreement with previously reported emission maxima wavelengths for NBD derivatives in hydrophilic environments (Rajarathnam et al., 1989; Rapaport and Shai, 1992). However, upon addition of the membranes to the solution of the NBD-labelled peptides (pH 6.8), a blue shift in the fluorescence emission maxima of all NBD-labelled peptides was observed (Table 2). No such shift could be detected using the control molecule NBD-aminoethanol. The change in its spectrum reflects the relocation of the NBD group into a more hydrophobic environment, i.e. within the lipidic environment of the membranes. For all of the NBD-labelled peptides, the extent of the blue shift is typical for relocalization of the probe into the hydrophobic core of the membrane, and it is different from that expected for surface localization ($\lambda_{max} = 533$ nm; Chattopadhyay and London, 1987). That the blue shift of NBD-α-5 ($\lambda_{max} = 524$ nm) is larger than that observed for NBD-Lys-α-5 ($\lambda_{max} = 527$ nm) suggests that the peptide is inserted into the lipidic core of the membranes with its N-part in a more hydrophobic environment than its C-terminal part.

Enzymic digestion of membrane-bound NBD-α-5 peptides

The susceptibility of membrane-bound NBD-labelled peptides to proteolytic digestion by proteinase-K was investigated. When NBD-α-5 and proteinase-K were co-incubated for 5–10 min, followed by their addition to a solution containing mid-gut

Table 1 Sequences of α-5 peptides and their fluorescently labelled analogues

No.	Modification		Peptide designation	Sequence
1	**X** = H	**Z** = H	α-5	**X**-HN-F[193] L T T Y A Q A A N T H L F L L K D A Q I Y G[215]-COOH
2	**X** = NBD	**Z** = H	NBD-α-5	
3	**X** = Acetyl	**Z** = NBD	NBD-Lys-α-5	NH-**Z**
4	X = H		P-α-5	**X**-HN-F[193] L T T Y A Q A **P** N T H L F L L K D A Q I Y G[215]-COOH
5	X = NBD		NBD-α-5	

Table 2 Emission maxima and relative fluorescence increases of NBD-labelled α-5 peptides upon interaction with mid-gut membranes

Peptide designation	Emission maximum in buffer (nm)	Emission maximum with membranes (nm)	$F_{membranes}/F_{buffer}$
NBD-α-5	549±1	524±1	6.8
NBD-Lys-α-5	549±1	527±1	5.3
NBD-P-α-5	549±1	525±1	6.3
NBD-ethanolamine	549±1	549±1	1.0

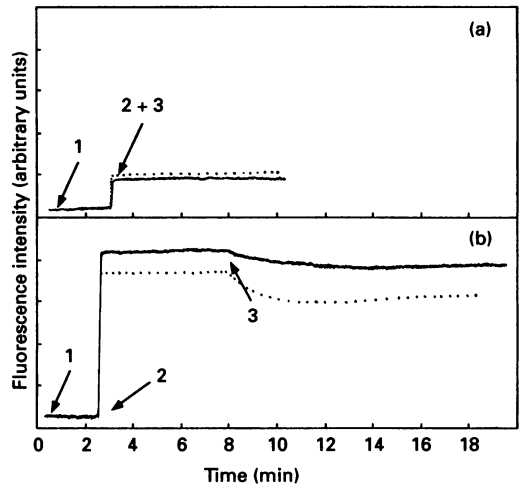

Figure 1 Digestion of NBD-α-5, NBD-Lys-α-5, and NBD-P-α-5 by proteinase-K

Mid-gut membranes (1.8 mg dry wt.; 1), NBD-peptide (0.1 μM; 2), and proteinase-K (5 μg; 3) were mixed together (final vol. 2 ml) in buffer composed of 50 mM Na_2SO_4, 25 mM Hepes/SO_4^{2-}, pH 6.8, and at room temperature, at the indicated times in the following order: (**a**) Membranes (1) and then a mixture of peptide (2) plus enzyme (3) preincubated for 5 min. (**b**) Membranes (1) then peptide (2) and finally enzyme (3). The excitation wavelength was set at 470 nm and the emission wavelength was monitored at 530 nm. Designations: solid, NBD-α-5; broken line, NBD-P-α-5.

membranes, the fluorescence intensity remained low (Figure 1a). Thus, once the NBD-α-5 was digested, addition of mid-gut membranes did not cause an increase in the fluorescence intensity of the NBD probe. This result indicated that enzymically cleaved α-5 did not bind to the membranes. Similar results were obtained with NBD-P-α-5 and NBD-Lys-α-5. In contrast, when NBD-α-5 was mixed with membranes prior to addition of the enzyme (Figure 1b), the fluorescence intensity of the NBD moiety increased. Only a small decrease (11%) in fluorescence occurred upon the addition of the enzyme, demonstrating that when bound to insect membranes, the majority of NBD-α-5 peptide was protected from digestion by proteinase-K. Similar results were obtained when membrane-bound NBD-Lys-α-5 was reacted with proteinase-K (10% decrease). However with NBD-P-α-5, a larger degree of enzymic cleavage occurred (26% decrease). These results were consistent with those obtained with a model membrane (Gazit and Shai, 1993), and may indicate that some population is exposed to the surface. The binding of both NBD-α-5 and NBD-P-α-5 seemed to be irreversible, since no additional cleavage was observed over a longer period of time. The degree of the enzymic cleavage observed therein was much lower than that obtained with peptides assumed to lie on the surface of the membrane such as the anti-bacterial dermaseptin (Pouny et al., 1992).

Single channel formation by α-5 in planar bilayers (PLMs)

The ability of α-5 peptide to induce single channels in PLMs composed of soybean lecithin + 20% (w/w) cholesterol, and at pH 7.4, was assessed. Channel activity was induced by addition of α-5 [dissolved either in IPA/H_2O (1:1, v/v) or in TFE/H_2O (1:1, v/v)] on one side of preformed bilayers (virtual ground). The salt solutions were either 0.5 M NaCl or 0.5 M KCl both in 5×10^{-3} M Hepes, pH 7.4. Similar results have been obtained independently of the solvents or salt composition used. The process of channel formation is rather complex. Addition of α-5 to the solution at various concentrations results in formation of small, irregular current fluctuations of low amplitude (about 2–5 pS) which stay open for several tens of milliseconds. With time, both the amplitude and the open time increase and the channel traces become more regular, with characteristic rectangular shapes. Figure 2 shows representative single channel traces. The traces were obtained at a trans-negative potential of −20 mV, and were filtered at 100 Hz. As seen in the Figure the size of the conductance fluctuations and the open time of the single channels were variable. Single channel traces of a continuous recording of 2 min duration were analysed and used for the construction of histograms of current amplitudes (Figure 3). A fit of the histogram data by three Gaussian distributions gave the most probable values of the conductance as 170, 300 and 445 pS. As the computer programs employed enabled us to discern the various current levels with better accuracy, this technique was also used and gave an additional conductance value of 30 pS (results not shown). It should be mentioned that occasionally higher conductances were obtained, with the highest value reaching 1000 pS. These conductance levels might be multiples of a single, low conductance level indicating simultaneous opening of several channels. Alternatively, they might be explained by the formation of aggregates composed of variable

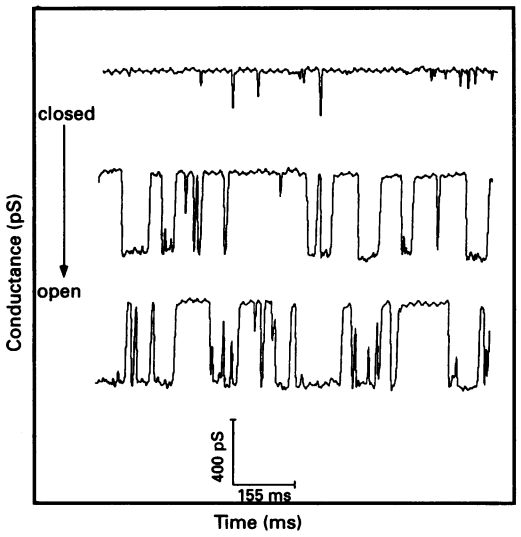

Figure 2 Single channel traces for α-5

Representative traces of single channels formed by α-5 (16 μg/ml) in soybean lecithin bilayers in 0.5 M NaCl buffered with 5 mM Hepes, pH 7.4. The applied potential was −20 mV and the traces were filtered at 100 Hz.

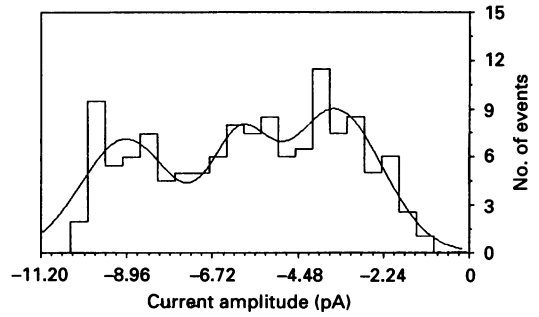

Figure 3 Current amplitude histograms

Current amplitude histograms derived from a 2 min recording. The histograms were constructed from traces similar to those in Figure 2, and fitted by three Gaussian distributions giving the most probable values of the conductance as 170, 300, and 445 pS (259 points).

numbers of α-5 monomers, associating and dissociating at various rates. The heterogeneity of the conductance values (200–4000 pS in 0.3 M KCl) was also reported by Slatin et al. (1990) for the channels formed by Bt CryIIIA and CryIA$_c$ δ-endotoxin proteins.

The aim of the single channel experiments was to give further support to the hypothesis that α-5 monomers can form stable aggregates within the membrane. Simple association of peptide with the surface of the bilayer, leading to bilayer distortion and 'detergent-like' effects, would not be expected to produce rectangular conductance traces such as those observed. However, it is not claimed that α-5 is the only channel-lining segment. Therefore, selectivity experiments were not conducted, and were beyond the scope of the present study.

Cytotoxic activity of α-5 and P-α-5

The *in vitro* toxicity of α-5 or P-α-5 to Sf-9 insect cells was determined. The peptides at increasing concentrations were added

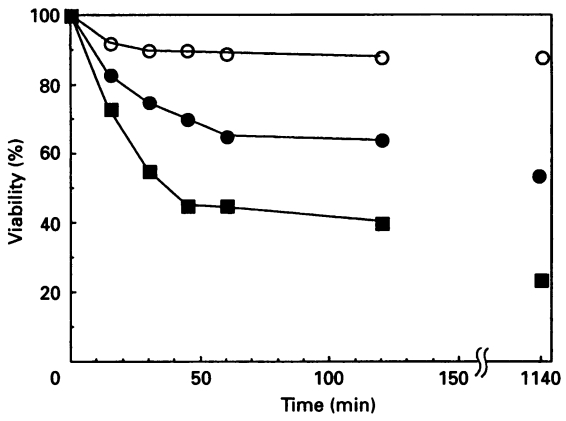

Figure 4 Cytotoxic activity of α-5 and P-α-5 towards insect Sf-9 cells

Peptides dissolved in DMSO were added to cells (approx. 6×10^4 cells/well) at a concentration of 50 μg/ml. Viability was monitored with time at room temperature and was measured by Trypan Blue (0.1%, w/v) vital staining assay. Symbols: ■, α-5; ●, P-α-5; ○, DMSO alone.

Table 3 Geometric and energetic analysis of α-5 helix bundle models

Comparison of parallel ($\Omega_{INIT} = 0°$) and tilted ($\Omega_{INIT} = +18°$) helix models of hexameric α-5 helix bundles. Inter-helix crossing angles (Ω), separations (R), helix–helix interaction energies (ΔE^{VDW} and ΔE^{ES}), and changes in accessible surface area upon bundle formation (ΔA) are given as a mean ± S.D. for each ensemble of 16 structures.

Model	$\Omega_{INIT} = 0°$	$\Omega_{INIT} = +18°$
Ω (°)	+7.2 (2.5)	+15.5 (1.6)
R (Å)	9.6 (0.3)	9.3 (0.4)
ΔE^{VDW} (kcal/mol)	−134 (31)	−181 (39)
ΔE^{ES} (kcal/mol)	−309 (9)	−332 (14)
ΔA (Å^2)	7670 (110)	7950 (170)

to the cells. A significant cytotoxic effect was observed at a peptide concentration of 10 μg/well (50 μg/ml). Therefore, this concentration was selected to follow the viability of the cells with time. In control experiments the solvent alone was used. Monitoring of viability was performed using Trypan Blue staining. Figure 4 shows the time-dependent viability of the cells in the presence of the peptides (10 μg/well) or the solvent alone. As seen in the Figure, α-5 is more cytotoxic to the cultured cells than P-α-5. This is in agreement with the lower affinity of P-α-5 for model phospholipid membranes, and with its lower α-helical content in hydrophobic environments relative to α-5 (Gazit and Shai, 1993). Similar cytotoxic effects and changes in the shape of the cells have been reported previously using δ-endotoxins at a concentration of 25 μg/ml (Thomas and Ellar, 1983). Interestingly, the lower cytotoxicity of P-α-5 as compared with that of α-5 correlates with the low cytotoxic potency observed with site-directed mutants of CryIA$_c$ (Wu and Aronson, 1992) and *sotto* (Ahmad and Ellar, 1990) δ-endotoxins, in which prolines substitute alanines at the same or nearby positions within their α-5 segments.

Molecular modelling

Hexameric bundles have been generated as described above. Geometric and energetic analysis of the two classes of model are summarized in Table 3. For both values of Ω_{INIT} the final helix

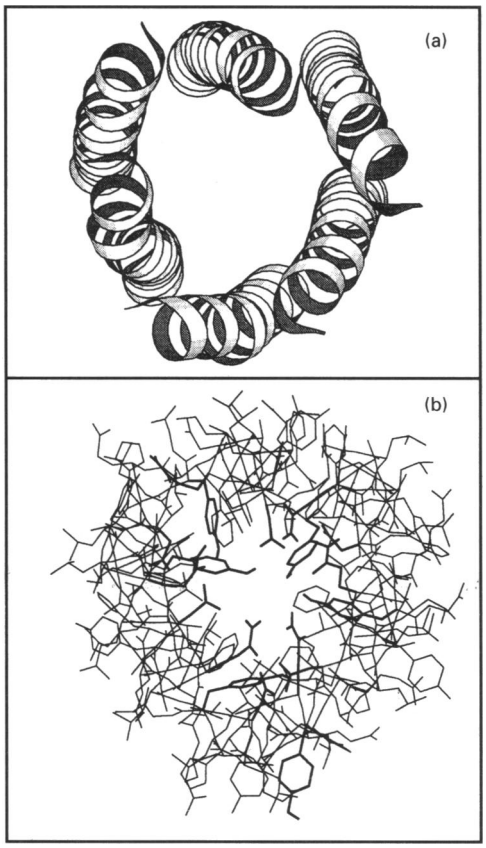

Figure 5 Model of an $n = 6$ bundle of α-5 helices, generated by SA/MD using $\Omega_{INIT} = +18°$

(**a**) Helices of the bundle in a 'ribbon' representation, illustrating the left-handed coiled coil formed by the helices. (**b**) All of the heavy atoms of the model. The side chains of residues Q199, D210 and Y214 are highlighted. Note the possibility of alternative conformations of the Y214 side chain. In this model, three of the six Y214 side chains form part of the pore lining.

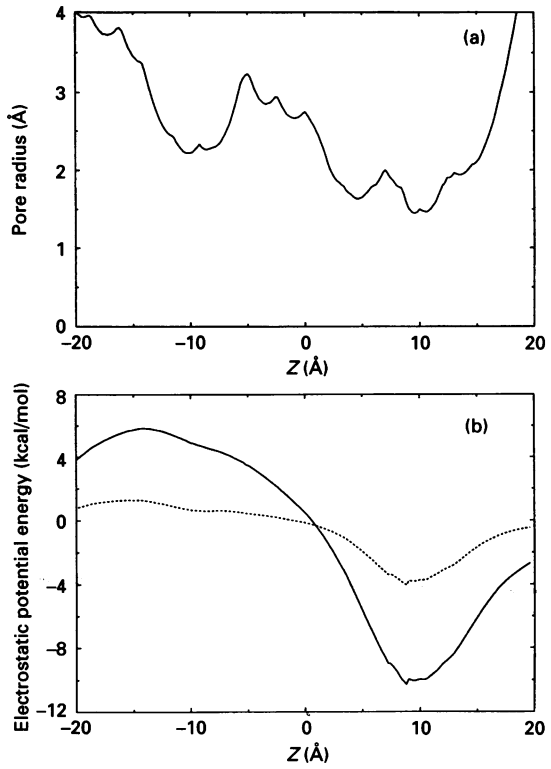

Figure 6 Analysis of the pore through the centre of the helix bundle shown in Figure 5

(**a**) Pore radius as a function of distance along the z (i.e. pore) axis, calculated using HOLE. (**b**) Electrostatic potential energy as a function of z, for points along the pore defined by HOLE. Two potential profiles are shown, one corresponding to zero ionic strength (continuous line) and the other corresponding to an ionic strength of 500 mM (broken line). Conversion factors: 1 Å = 0.1 nm; 1 cal ≈ 4.185 J.

crossing angle is positive, corresponding to left-handed coiled coil structures (Cohen and Parry, 1990). Interestingly, the X-ray structure of a tetrameric bundle of synthetic GCN4-derived peptides exhibits a left-handed coiled coil (Harbury et al., 1993), as do SA/MD-derived models of bundles formed by simple hydrophobic and amphipathic transmembrane helices (Kerr et al., 1994). The final value of R is somewhat lower for the $\Omega_{INIT} = +18°$ (i.e. tilted helix) model, suggesting closer packing of the helices. This is supported by analysis of the potential energy of interaction of the helices, $\Delta E = E(\text{bundle}) - E(\text{constituent helices})$. Evaluation of the surface area buried upon formation of the bundles (ΔA) reveals that the buried areas per monomer (1280 Å^2 and 1325 Å^2 for the parallel and tilted bundle models respectively) are comparable with that observed in the crystal structure of tetrameric melittin (1040 Å^2; Janin et al., 1988).

On this basis of the greater interaction energy and larger buried surface area of the tilted helix model, this last ensemble has been explored in more detail as a plausible model of $n = 6$ α-5 channels. Two representations of a structure from the tilted helix ensemble are shown in Figure 5. The left-handed coiled coil (pitch 300 Å) is evident in Figure 5(a). For some structures of the ensemble the pore has been occluded by the side chains of one or more Y214 residues. Comparison of the different structures suggests that changes in the conformation of the Y214 side chains might open or close the channel. Inspection of Figure 5(b) indicates multiple possible conformations for Y214. The side chains of residues Q199, T203, D210 and Y214 provide a hydrophilic lining to the pore. This is of some interest given recent studies of possible cation–π interactions in the pore region of voltage-gated potassium channels (Gao et al., 1993; Kumpf and Dougherty, 1993).

The pore radius as a function of distance along the z (i.e. pore)-axis was evaluated for all members of the ensemble, using HOLE (Smart et al., 1993; Kerr et al., 1994). Similar profiles were seen for all members of the ensemble, differing mainly in their exact radii in the vicinity of constrictions of the pore. The structure shown in Figure 5 was selected as having the highest minimum pore radius. The pore radius profile for this structure is shown in Figure 6(a). The N-termini of the helices at z are about −20 Å and the C-termini at z are about +15 Å. The mean radius of the pore is about 2.5 Å. Constrictions occur at $z = -10$ Å (where the closest contact is with atom Oϵ1 of residue Q199), at $z = +5$ Å (Cδ1:L207) and at $z = +10$ Å (Oη:Y214). The Y214 contact results in a minimum pore radius of 1.5 Å. This is greater than the radius of an isolated K^+ ion (1.33 Å) but somewhat less than the radius of a hydrated K^+ ion (1.7 Å; Moore, 1972), suggesting that this structure is a reasonable representation of at least one of the conductance levels of the α-5 channels.

Electrostatic properties of the pore were estimated using the

UHBD program (Davis et al., 1991) to evaluate an electrostatic potential energy for a +1 probe charge at each point along the pore defined by the HOLE trajectory (Figure 6b). Solvent and protein dielectrics of 78 and 2 respectively were employed, and the calculation was performed for ionic strengths of 0 and 500 mM (the latter corresponding to that employed in the ion channel measurements). At 0 mM the potential profile was dominated by the aligned helix dipoles of the bundle. At 500 mM the helix dipole effect was screened, revealing the electrostatic potential profile of the interior of the pore. The main feature was a minimum at a z of about +8–10 Å. This corresponded to the D210 side chains at a z of about +9 Å, and suggested that these side chains might act as a selectivity filter for α-5 channels, favouring permeation by cations. There was also a small dip in the profile at a z of about −8 Å corresponding to the Q199 side chains.

DISCUSSION

The major toxic effect of δ-endotoxins is proposed to be the formation of pores in the mid-gut epithelium of insects, which ultimately leads to their death. The α-5 helix of these proteins was proposed to play a major role in their toxic mechanism, probably by being a constituent of a bundle of trans-membrane α-helices which are thought to form the pore (Ahmad and Ellar, 1990; Wu and Aronson, 1992). The existence of a cleavage site between α-5 and α-6 further strengthens this proposal (Angsuthanasombat et al., 1993) We have shown recently that a peptide with a sequence identical to that of α-5 has structural and permeation properties (Gazit and Shai, 1993) similar to those of toxins such as mellitin (Morgan et al., 1983; Murata et al., 1987) the shark repellent neurotoxin pardaxin (Shai et al., 1990, 1991) and various anti-microbial peptides (Steiner et al., 1988; Pouny et al., 1992). Whether α-5 has *in vitro* activities and whether its permeation properties result from membrane destabilization or channel formation was further investigated herein.

The ability of α-5 to interact with insect mid-gut membranes was demonstrated by utilizing NBD-α-5, labelled at two different sites (Table 2). The existence of a difference in the environment encountered by NBD located at the N-part versus the C-part of α-5 argues in favour of α-5 existing in an organized manner within the acyl-chain region of the membrane, rather than in a random distribution. Furthermore, if we assume that α-5 forms aggregates, as proposed by the shape of its binding isotherms (Gazit and Shai, 1993), and by its ability to form single channels (Figure 2), then this reflects the preferential organization of the α-5 monomers within the aggregates in a parallel manner. The aggregates are probably inserted into the membrane through their N-terminal, since it has the ability to penetrate into the lipid core of the membrane (λ_{max} = 524 nm) (Chattopadhyay and London, 1987). Membrane-bound α-5 peptides are also protected from proteolytic digestion by proteinase-K (Figure 1) which also supports the assumption that membrane-associated α-5 is localized within the lipid bilayers. However, although less favoured, the resistance towards proteolysis could also be explained by a conformational change of the peptide from a predominantly random coil structure in aqueous solution to an α-helical structure in a hydrophobic environment (Gazit and Shai, 1993). Indeed, the c.d. spectra of α-5 in methanol have revealed high α-helical content, while that of P-α-5 is a reduced one (Gazit and Shai, 1993). Various studies have shown a direct correlation between the structure of amphipathic polypeptides in methanol and in the presence of phospholipid membranes (Kelsh et al., 1992). The binding isotherms of both α-5 and P-α-5 have revealed that the lipid/peptide molar ratio required for having a high concentration of bound peptide is high (> 3000:1) (Gazit and Shai, 1993). When c.d. experiments were conducted under such conditions significant light scattering occurred even in the case of small unilamellar vesicles, and the results could not be interpreted. In other studies, where c.d. studies could be conducted also in the presence of vesicles, most peptides were bound at a lipid/peptide molar ratio of 200–800:1. In these cases similar results were obtained whether methanol, 40% TFE or phospholipid vesicles were utilized (Shai et al., 1990; Pouny and Shai, 1992).

The cytotoxicity of α-5 to Sf-9 insect cells *in vitro*, and that P-α-5 is less cytotoxic than α-5 (Figure 4), correlates with the *in vivo* and *in vitro* marked decrease in the toxicity of site-directed mutants of CryIAc (Wu and Aronson, 1992) and *sotto* (Ahmad and Ellar, 1990) δ-endotoxins, in which prolines substitute the alanines at the same or nearby positions within their α-5 segments. This further suggests a role for α-5 in the toxic mechanism of δ-endotoxins.

It has been shown that Bt δ-endotoxins form ion channels in planar lipid bilayers (Slatin et al., 1990; Schwartz et al., 1993). The channels have exhibited several conductance levels ranging from 100 pS to about 4000 pS. The ability of α-5 to form single channels supports a role for α-5 as a transmembrane segment which can form organized transmembrane bundles of amphiphilic α-helices, with their outwardly directed hydrophobic surfaces interacting with the lipidic constituents of the membrane, and inwardly facing hydrophilic surfaces producing a pore; a model proposed for other proteins as well (Inouye, 1974; Guy and Seethharamulu, 1986; Oiki et al., 1988a,b; Tosteson et al., 1987; Ghosh and Stroud, 1991; Grove et al., 1991; Langosch et al., 1991; Sansom, 1991; Rapaport et al., 1992). A channel-like bundle formed by α-5 has been further supported by molecular modelling used to generate a plausible channel formed by hexameric (n = 6) bundles of α-5 helices (Figure 5). Almost certainly, channels with other values of n are also formed. The computational work is not offered as proof that α-5 can form a helix bundle, but rather as a model of the structure of such a bundle. The geometric and electrostatic properties of such models are thus explored in the context of their possible involvement in ion channel formation. Interestingly, the channels formed by α-5 have similar kinetics and conductance properties as observed for the whole protein (Figures 2 and 3). These results support our previous hypothesis, based on the upper curvature of the binding isotherms of α-5 (Gazit and Shai, 1993), that the peptide can insert into phospholipid membranes and form aggregates therein. The heterogeneity of the channel conductance observed with α-5 (Figure 2) might be explained by the association of different numbers of monomers in the peptide aggregates that form the channels. Thus, the various conductances may reflect a difference in the multimeric state of the peptide forming the channel. A second possible source of conductance heterogeneity lies in alternative conformations of channel-lining side chains (e.g. Y214), as suggested by the modelling studies. The conductance increases with time as more monomers diffuse from the solution to the bundle of the α-helices, or reach the channel by lateral diffusion in the plane bilayer. A heterogeneity of channel conductance has also been observed with other channel-forming peptides such as the δ-toxin from *Staphylococcus aureus* (Mellor et al., 1988), the M2-δ segment of the nicotinic cholinergic receptor (Oiki et al., 1988a), the MA-β peptide corresponding to a segment of the nicotinic acetylcholine receptor (Ghosh and Stroud, 1991), and the transmembrane segment of the minK potassium channel (Ben-Efraim et al., 1993). From the reported properties of α-5 it is by no means aimed to claim that the segment is the only pore-lining segment of the toxin, but rather

that α-5 can be stabilized within the membrane by forming bundles of helices. In the presence of the other helices of the protein heteroaggregates might be favoured as well. Current models explaining δ-endotoxin's toxicity (review by Gill et al., 1992) assign two major domains in the toxin, one involved in receptor binding and one responsible for their toxic effects. Receptor binding probably causes conformational changes, thus exposing δ-endotoxin's pore-forming domain, which contains the α-5 helix. The subsequent interaction of the toxic domain with target cell membranes probably involves two important steps: (i) non-specific protein–lipid interaction; and (ii) protein–protein interaction within the membrane to form an assembly of α-helices which form a pore (see, for example, Parker and Pattus, 1993). Since α-5 fulfils these two criteria, i.e. interacts with membranes and forms bundles therein, it may at least be one of the helices which contributes to these processes.

Taken together, the results presented here provide further support for the hypothesis that α-5 is a structural component of the pores formed by δ-endotoxins via aggregation of amphiphilic α-helices. These results also raise the possibility of local amino acid substitution in α-5 as a means of increasing its potency. Such altered α-5 sequences might then be inserted into α-endotoxins via site-directed mutagenesis to form more active toxins.

Note added in proof (received 14 October 1994)

A homologous extended version of the α-5 segment from CryIA(c) has recently been shown to form single channels in planar lipid membranes, thus supporting our findings (Cummings et al. 1994).

We thank Professor Baruch Sneh for providing us with the mid-gut membranes and Dr. Aviah Zilberstein for helpful discussions. We acknowledge the support of the Oxford Centre for Molecular Science in making available computational facilities for the modelling studies. This research was supported in part by the Israel Cancer Association, and by the Basic Research Foundation administered by the Israel Academy of Sciences and Humanities, the Wellcome Trust and the U.K. Science and Engineering Research Council. Y.S. is incumbent of the Adolpho and Evelyn Blum Career Development Chair in Cancer Research.

REFERENCES

Ahmad, W. and Ellar, D. J. (1990) FEMS Microbiol. Lett. **68**, 97–104
Angsuthanasombat, C., Crickmore, N. and Ellar, D. J. (1993) FEMS Microbiol. Lett. **111**, 255–262
Aronson, A. I. (1993) Mol. Microbiol. **7**, 489–496
Ben-Efraim, I., Bach, D. and Shai, Y. (1993) Biochemistry **32**, 2371–2377
Brasseur, R. (1991) J. Biol. Chem. **266**, 16120–16127
Brünger, A. T. (1993) X-PLOR, Version 3.1, A system for X-ray crystallography and NMR, Yale University Press, New Haven, CT
Chattopadhyay, A. and London, E. (1987) Biochemistry **26**, 39–45
Chothia, C., Levitt, M. and Richardson, D. (1981) J. Mol. Biol. **145**, 215–250
Cohen, C. and Parry, D. A. D. (1990) Proteins: Struct. Funct. Genet. **7**, 1–15
Coronado, R. and Latorre, R. (1983) Biophys. J. **43**, 231–236
Cummings, C. E., Armstrong, G., Hodgman, T. C. and Ellar, D. J. (1994) Mol. Membr. Biol. **11**, 87–92
Davis, M. E., Madura, J. D., Luty, B. A. and McCammon, J. A. (1991) Comput. Phys. Commun. **62**, 182–197
Gao, J., Chou, L. W. and Auerbach, A. (1993) Biophys. J. **65**, 43–47
Gazit, E. and Shai, Y. (1993) Biochemistry **32**, 3429–3436
Ge, A. Z., Shivarova, N. I. and Dean, D. H. (1989) Proc. Natl. Acad. Sci. U.S.A. **86**, 4037–4041
Ghosh, P. and Stroud, R. M. (1991) Biochemistry **30**, 3551–3557
Gill, S. S., Cowles, E. A. and Pietrantonio, P. V. (1992) Annu. Rev. Entomol. **37**, 615–636
Greenblatt, R. E., Blatt, Y. and Montal, M. (1985) FEBS Lett. **193**, 125–134
Grove, A., Tomich, J. M. and Montal, M. (1991) Proc. Natl. Acad. Sci. U.S.A. **88**, 6418–6422
Guy, H. R. and Seetharamulu, P. (1986) Proc. Natl. Acad. Sci. U.S.A. **83**, 508–512
Harbury, P. B., Zhang, T., Kim, P. S. and Alber, T. (1993) Science **262**, 1401–1407
Hink, W. F. (1970) Nature (London) **226**, 466–467
Höfte, H. and Whiteley, H. R. (1989) Microbiol. Rev. **53**, 242–255
Inouye, M. (1974) Proc. Natl. Acad. Sci. U.S.A. **71**, 2396–2400
Janin, J., Miller, S. and Chothia, C. (1988) J. Mol. Biol. **204**, 155–164
Kagawa, Y. and Racker, E. (1971) J. Biol. Chem. **246**, 5477–5487
Kelsh, L. P., Ellena, J. F. and Cafiso, D. S. (1992) Biochemistry **31**, 5136–5144
Kerr, I. D. and Sansom, M. S. P. (1993) Eur. Biophys. J. **22**, 269–277
Kerr, I. D., Sankararamakrishnan, R., Smart, O. S. and Sansom, M. S. P. (1994) Biophys. J. **67**, 1501–1515
Knowles, B. H. and Ellar, D. J. (1987) Biochim. Biophys. Acta **924**, 509–518
Kraulis, P. J. (1991) J. Appl. Crystallogr. **24**, 946–950
Kumpf, R. A. and Dougherty, D. A. (1993) Science **261**, 1708–1710
Langosch, D., Hartung, K., Grell, E., Bamberg, E. and Betz, H. (1991) Biochim. Biophys. Acta **1063**, 36–44
Lear, J. D., Wasserman, Z. R. and De Grado, W. F. (1988) Science **240**, 1177–1181
Lee, M. K., Ross, E. M., Ge, A. Z. and Dean, D. H. (1992) J. Biol. Chem. **267**, 3115–3121
Li, J., Carroll, J. and Ellar, D. J. (1991) Nature (London) **353**, 815–821
Mellor, I. R., Thomas, D. H. and Sansom, M. S. P. (1988) Biochim. Biophys. Acta **942**, 280–294
Moore, W. J. (1972) Physical Chemistry (5th edn.), Longman, London
Morgan, D. G., Williamson, H., Fuller, S. and Hudson, B. (1983) Biochim. Biophys. Acta **732**, 668–674
Murata, M., Nagayama, K. and Ohnishi, S. (1987) Biochemistry **26**, 4056–4062
Nilges, M. and Brünger, A. T. (1991) Protein Engineer. **4**, 649–659
Oiki, S., Danho, W., Madison, V. and Montal, M. (1988a) Proc. Natl. Acad. Sci. U.S.A. **85**, 2393–2397
Oiki, S., Danho, W. and Montal, M. (1988b) Proc. Natl. Acad. Sci. U.S.A. **85**, 8703–8707
Parker, M. W. and Pattus, F. (1993) Trends Biochem. Sci. **18**, 391–395
Pouny, Y. and Shai, Y. (1992) Biochemistry **31**, 9482–9490
Pouny, Y., Rapaport, D., Mor, A., Nicolas, P. and Shai, Y. (1992) Biochemistry **31**, 12416–12423
Rajarathnam, K., Hochman, J., Schindler, M. and Ferguson-Miller, S. (1989) Biochemistry **28**, 3168–3176
Rapaport, D. and Shai, Y. (1992) J. Biol. Chem. **267**, 6502–6509
Rapaport, D., Danin, M., Gazit, E. and Shai, Y. (1992) Biochemistry **31**, 8868–8875
Sacchi, V. F., Parenti, P., Hanozet, G. M., Giordana, B., Lüthy, P. and Wolfersberger, M. G. (1986) FEBS Lett. **204**, 218–225
Sansom, M. S. P. (1991) Prog. Biophys. Mol. Biol. **55**, 139–236
Schwartz, J.-L., Garneau, L., Masson, L., Savaria, D. and Brousseau, R. (1991) Biochim. Biophys. Acta **1065**, 250–260
Schwartz, J.-L., Garneau, L., Savaria, D., Masson, L., Brousseau, R. and Rousseau, E. (1993) J. Membr. Biol. **132**, 53–62
Shai, Y., Bach, D. and Yanovsky, A. (1990) J. Biol. Chem. **265**, 20202–20209
Shai, Y., Hadari, Y. R. and Finkels, A. (1991) J. Biol. Chem. **266**, 22346–22354
Slatin, S. L., Abrams, C. K. and English, L. (1990) Biochem. Biophys. Res. Commun. **169**, 765–772
Smart, O. S., Goodfellow, J. M. and Wallace, B. A. (1993) Biophys. J., **65**, 2455–2460
Steiner, H., Andreu, D. and Merrifield, R. B. (1988) Biochim. Biophys. Acta **939**, 260–266
Thomas, W. E. and Ellar, D. J. (1983) J. Cell Sci. **60**, 181–197
Tosteson, M. T., Levy, J. J., Caporale, L. H., Rosenblatt, M. and Tosteson, D. C. (1987) Biochemistry **26**, 6627–6631
Van Rie, J., McGaughey, W. H., Johnson, D. E., Barnett, B. D. and Van Mellaert, H. (1990) Science **247**, 72–74
Wu, D. and Aronson, A. I. (1992) J. Biol. Chem. **267**, 2311–2317

Received 5 November 1993/16 June 1994; accepted 8 July 1994